Electronic Supplementary Information

Ionic Liquid-Assisted Hydrothermal Valorization and Redox Site Engineering of Spruce Cone Biowaste for High-Performance Heteroatom-Doped and Ceria-Modified Electrodes for Sustainable Supercapacitor Applications

Khadija Chaudhary[a,b], Adeen Ilyas[c], Tomáš Zelenka[a], Hidetsugu Shiozawa[b,d] Muhammad Farooq Warsi[e], Eric W. Cochran[c]*, and Sonia Zulfiqar[a,f]*,

[a]*Department of Chemistry, Faculty of Science, University of Ostrava, 30. Dubna 22, Ostrava, 701 03, Czech Republic*

[b]*J. Heyrovsky Institute of Physical Chemistry, Czech Academy of Sciences, Dolejskova 3, 182 23 Prague 8, Czech Republic*

[c]*Department of Chemical and Biological Engineering, Iowa State University, Sweeney Hall, 618 Bissell Road, Ames, Iowa 50011, USA*

[d]*Faculty of Physics, University of Vienna, Boltzmanngasse 5, 1090 Vienna, Austria*

[e]*Institute of Chemistry, Baghdad-ul-Jadeed Campus, The Islamia University of Bahawalpur, Bahawalpur, 63100, Pakistan*

[f]*Department of Physical Sciences, Lander University, 320 Stanley Ave, Greenwood, South Carolina 29649, USA*

Corresponding authors: ecochran@iastate.edu; szulfiqar@lander.edu

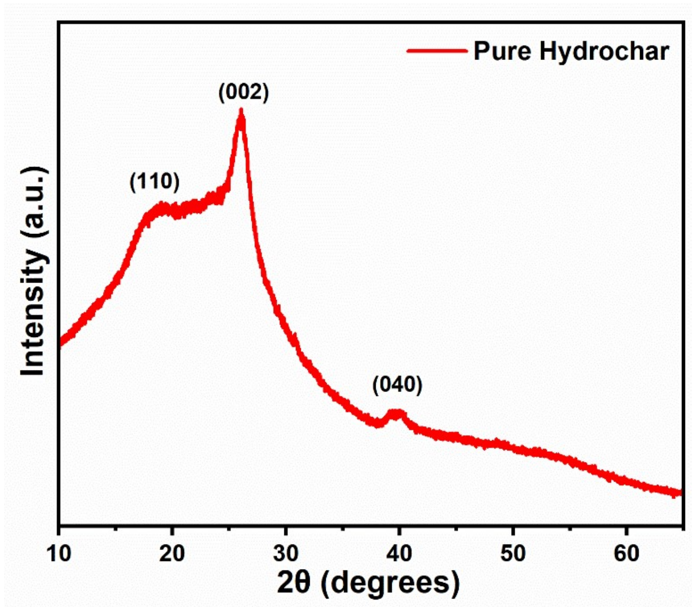

Figure S1. XRD pattern of pure hydrochar.

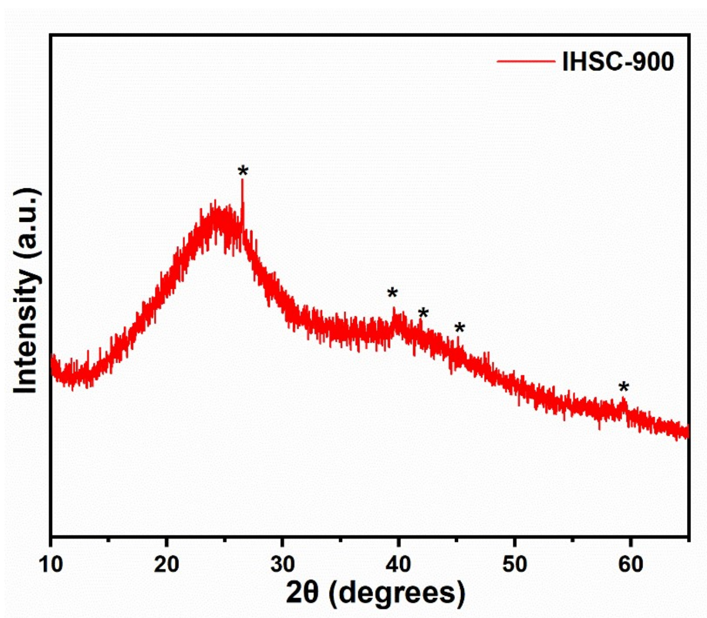

Figure S2. XRD pattern of IHSC-900 showing Fe impurities.

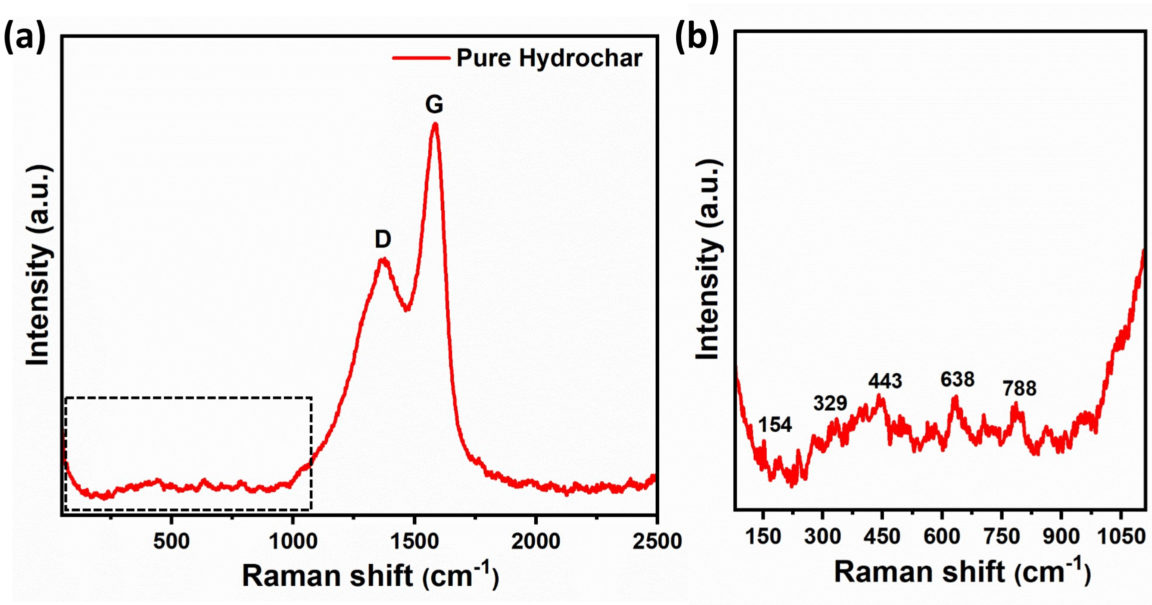

Figure S3. Raman spectrum of pure hydrochar.

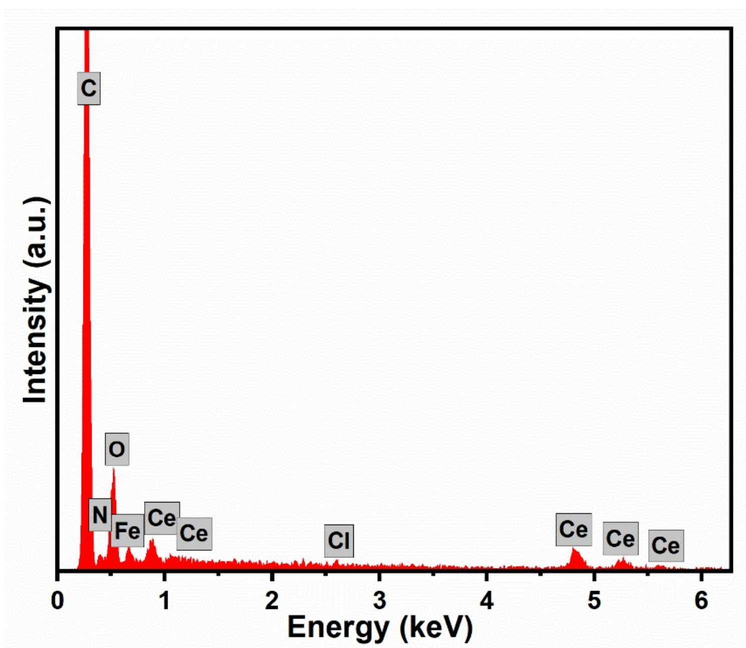

Figure. S4. EDX spectrum of Ce-IHSC-900.

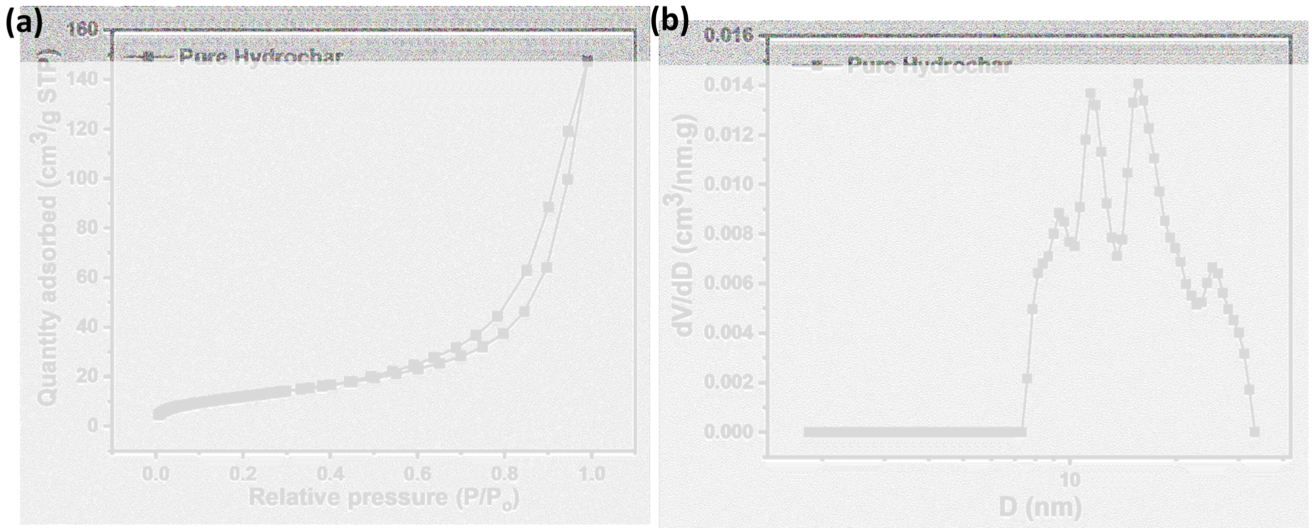

Figure S5. (a) N_2 adsorption-desorption plot (b) pore size distribution plot of pure hydrochar.

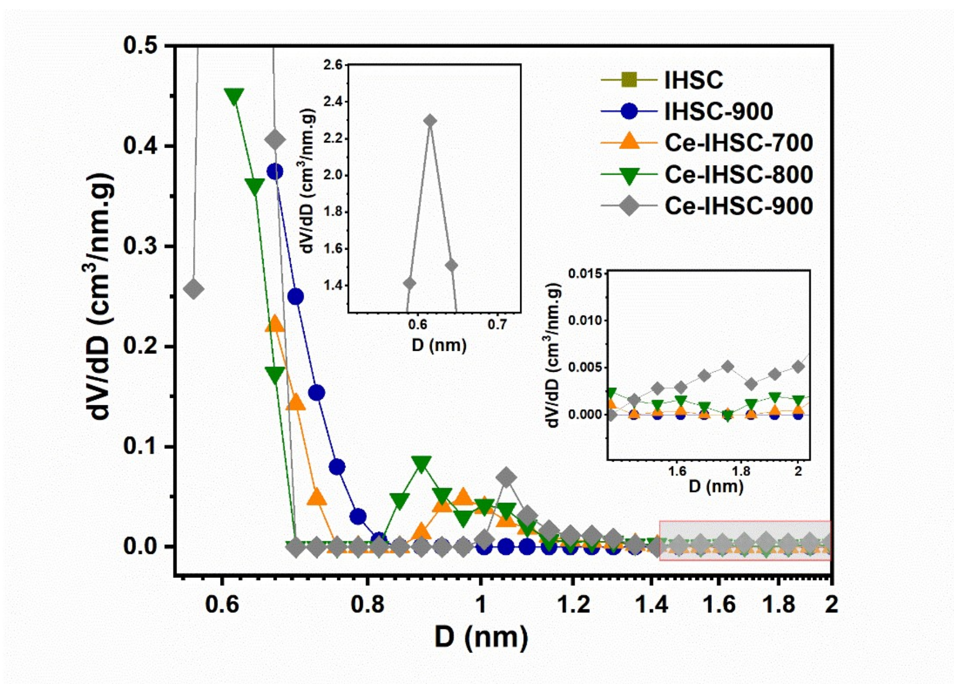

Figure S6. A close view of the micropore region of prepared hydrochars.

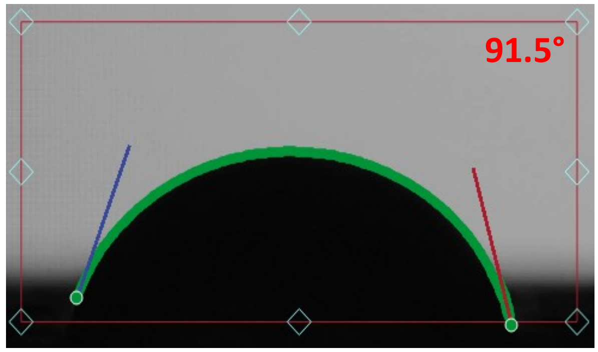

Figure S7. Contact angle among pure hydrochar and KOH electrolyte

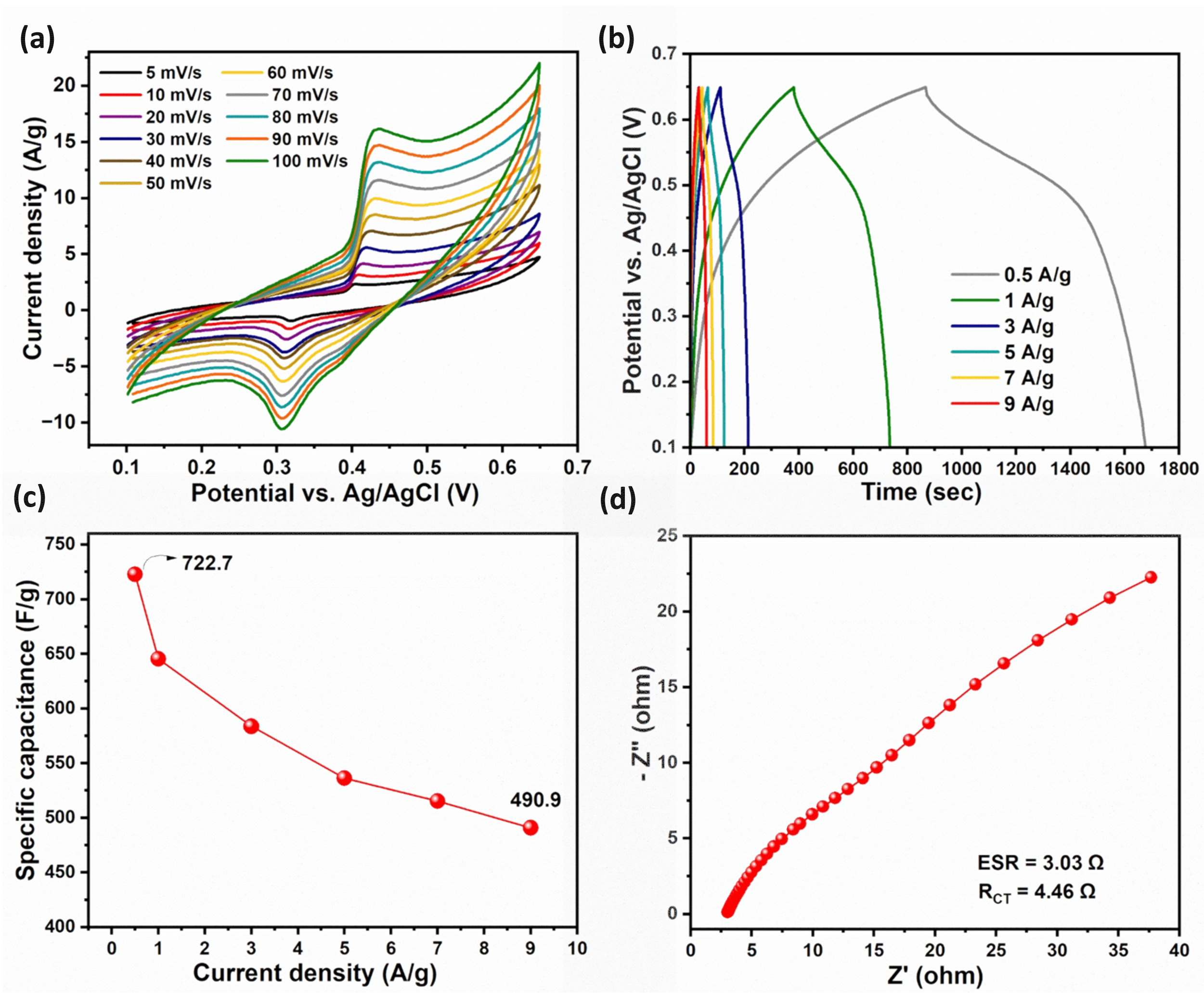

Figure S8. Electrochemical measurements of ceria modified hydrochar prepared in absence of [Bmim][$FeCl_4$]: (a) CV profiles at different scan rates (5-100 mV/s), (b) GCD plots at various current densities (0.5-9 A/g), (c) plot showing specific capacitance at different current density, and (d) Nyquist plot derived from EIS.

Table. S1. Elemental composition of hydrochars.

Hydrochars	EDX Wt.%					
	C	**O**	**N**	**Ce**	**Fe**	**Cl**
IHSC-900	74.6	21.22	1.24	-	2.31	0.63
Ce-IHSC-700	51.21	16.43	0.87	29.06	1.95	0.48
Ce-IHSC-800	53.29	14.4	0.92	28.87	1.97	0.55
Ce-IHSC-900	56.69	10.31	1.19	29.13	2.09	0.59

Table S2. Comparison of specific electrochemical performance of our synthesized hydrochar with already reported biomass-derived carbon electrodes.

Material	**Metal Oxide**	**Carbon source**	**Specific capacitance**	**Cyclic stability**	**Reference**
Ce-IHSC-900	CeO_2	Spruce cone	992.7 F/g at 0.5 A/g	95.2% after 7000 cycles	This work
ITC-JG-900	-	Juggan Grass	336 F/g at 1 A/g	88% after 2000 cycles	[1]
HC-MgO-700	MgO	Hazelnut shells	323 F/g at 1 A/g	80% after 4000 cycles	[2]
RSN-700	-	Rice Straw	400 F/g at 0.1 A/g	94.6% after 10,000 cycles	[3]
H-SDC-A650	-	Soybean	435 F/g at 0.5 A/g	91% after10,000 cycles	[4]
N-PCNS	-	Lactose monohydrate	263 F/g at 1 A/g	96% after 10,000 cycles	[5]
CPA-35-150	NiO-CoO	Corncob	208.5 F/g at 1 A/g	97.2 after 20,000 cycles	[6]
MnO_2-BP@PAni	MnO_2	Banana Peel	512.8 F/g 1 A/g	86.89% after 10,000 cycles	[7]
BPC/Fe_2O_3	Fe_2O_3	Wheat straw	987.9 F/g 1 A/g	82.6% after 3000 cycles	[8]
NiNF@TBC	$Ni(OH)_2$	Tea leaves	945 F/g 1 A/g	95% after 10,000 cycles	[9]
NiO@PC	NiO	Wheat husk	849 F/g 3 A/g	78% after 8000 cycles	[10]

References

1. Liu, Y., et al., *Biomass-derived hierarchical porous carbons: boosting the energy density of supercapacitors via an ionothermal approach.* Journal of Materials Chemistry A, 2017. **5**(25): p. 13009-13018.
2. Sinan, N. and E. Unur, *Hydrothermal conversion of lignocellulosic biomass into high-value energy storage materials.* Journal of energy chemistry, 2017. **26**(4): p. 783-789.
3. Jin, H., et al., *Three-dimensional interconnected porous graphitic carbon derived from rice straw for high performance supercapacitors.* Journal of Power Sources, 2018. **384**: p. 270-277.
4. Li, Z., et al., *Sustainable biowaste strategy to fabricate dual-doped carbon frameworks with remarkable performance for flexible solid-state supercapacitors.* Journal of Power Sources, 2019. **418**: p. 112-121.
5. Wang, Z., et al., *Large-scale fabrication of N-doped porous carbon nanosheets for dye adsorption and supercapacitor applications.* Nanoscale, 2019. **11**(18): p. 8785-8797.
6. Ai, J., et al., *Corncob cellulose-derived hierarchical porous carbon for high performance supercapacitors.* Journal of Power Sources, 2021. **484**: p. 229221.
7. Hamadi, F.Z., et al., *Synthesis and performance evaluation of supercapacitor based on banana peel–derived biochar loaded manganese dioxide with polyaniline ternary composite.* Ionics, 2024: p. 1-14.
8. Fang, K., et al., *Decorating biomass-derived porous carbon with Fe2O3 ultrathin film for high-performance supercapacitors.* Electrochimica Acta, 2018. **261**: p. 198-205.
9. Khedulkar, A.P., et al., *Flower-like nickel hydroxide@ tea leaf-derived biochar composite for high-performance supercapacitor application.* Journal of colloid and interface science, 2022. **623**: p. 845-855.
10. Zhang, S., et al., *NiO nanosheets anchored on honeycomb porous carbon derived from wheat husk for symmetric supercapacitor with high performance.* Journal of Alloys and Compounds, 2018. **735**: p. 1722-1729.